

Experimental studies and multiscale modeling of latent tracks in radiation-resistant insulators

FLNR JINR

V.A. Skuratov, R. Rymzhanov, A.E.Volkov, A.Ibrayeva, N.S.Kirilkin

Institute of Physics, Czech Academy of Sciences, Prague, Czech Republic

N.Medvedev

Centre for HRTEM, Nelson Mandela University, Port Elizabeth, South Africa

J.H.O'Connell, A. Janse van Vuuren, J. Neethling.

Institute of Nuclear Physics, Nur-Sultan, Kazakhstan

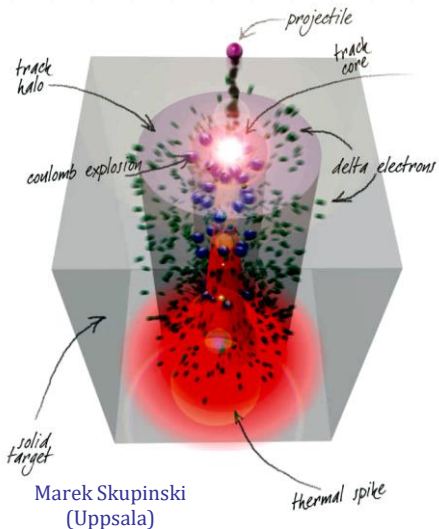
M.V.Zdorovets



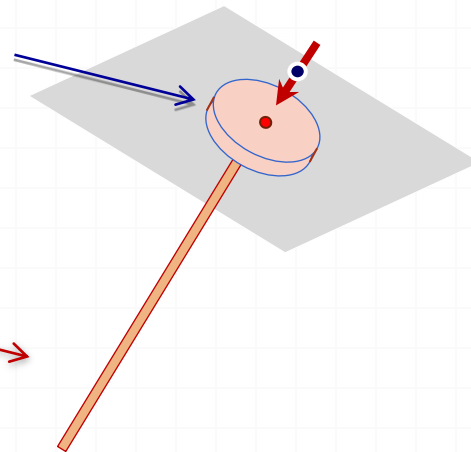
INSTITUTE OF NUCLEAR PHYSICS

of MINISTRY of ENERGY of the REPUBLIC of KAZAKHSTAN

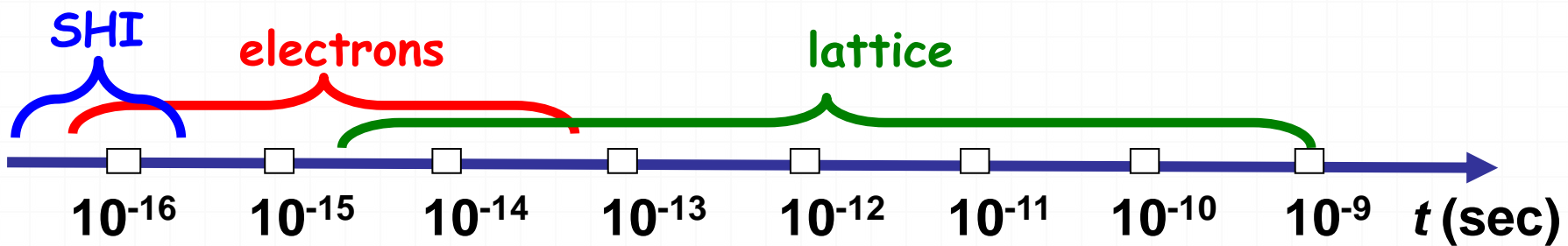
SHI track: temporal and spatial scales



Laser spot (1x1
μm)



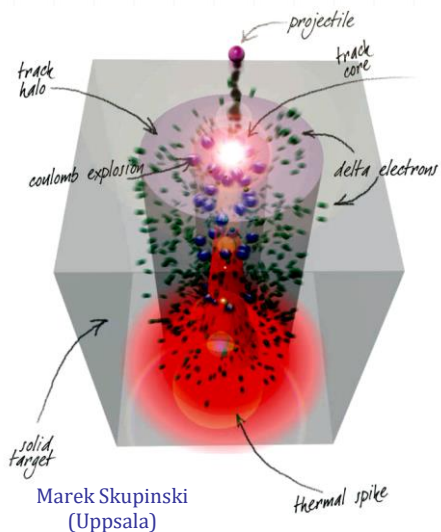
SHI Track
10nm x
100μm



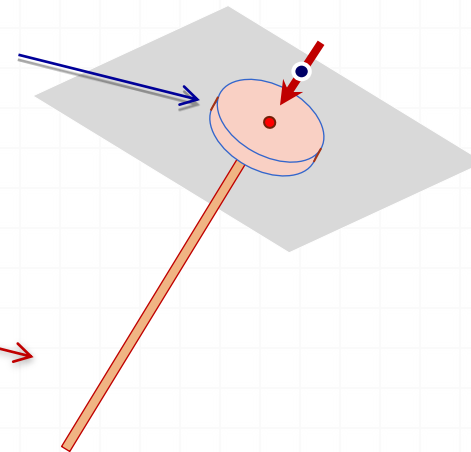
Too fast, too small, too large excitation levels

Can not be described with macroscopic models

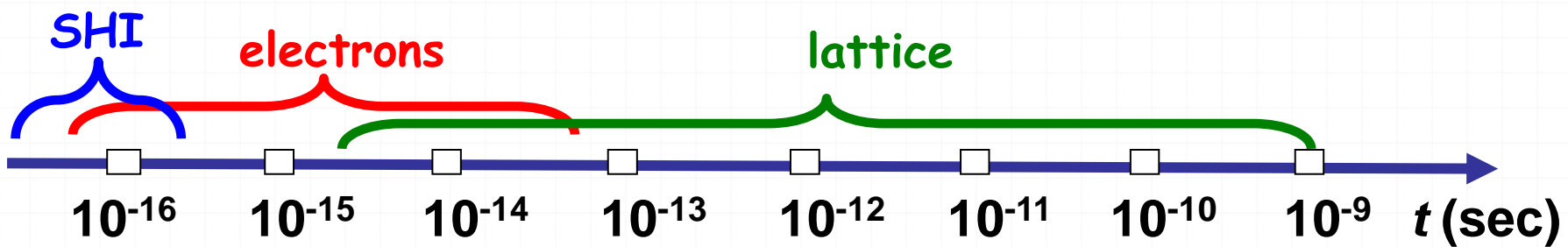
SHI track: temporal and spatial scales



Laser spot (1x1
μm)



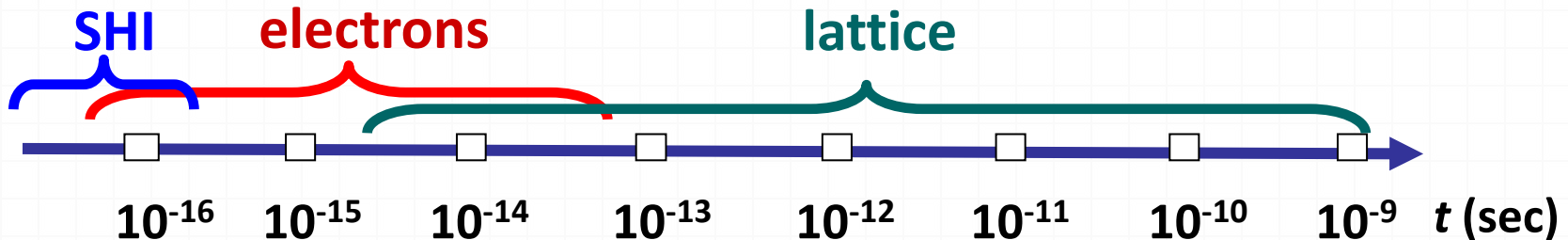
SHI Track
10nm x
100μm



Too fast, too small, too large excitation levels

Can not be described with macroscopic models

Multiscale microscopic model of track excitation



1. Monte Carlo of electronic excitations (10^{-14} s)

Spatial and temporal distributions of holes, fast electrons, their energies and momenta



2. A model of electron-lattice coupling and lattice excitation (10^{-12} s)

Spatial and temporal distributions of energy and momenta transferred into the lattice



3. MD of lattice relaxation (10^{-9} s)

Structure transformations



Monte Carlo (TREKIS) of the initial electronic kinetics

Time-Resolved Electron Kinetics in SHI Irradiated Solids

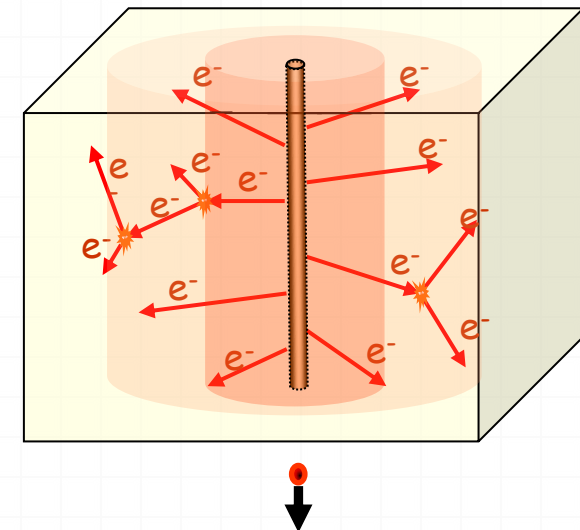
N.A.Medvedev et al., J. Phys. D Appl. Phys. 48 (2015) 355303

$$t = 10^{-17} \text{ s} - 10^{-14} \text{ s}$$

Event by event simulations

Scattering on spatially and dynamically coupled particles

$$\frac{\partial^2 \sigma}{\partial \Omega \partial(h\omega)} \sim |V(\mathbf{k})|^2 \operatorname{Im} \left(\frac{-1}{\varepsilon(k, \omega)} \right)$$



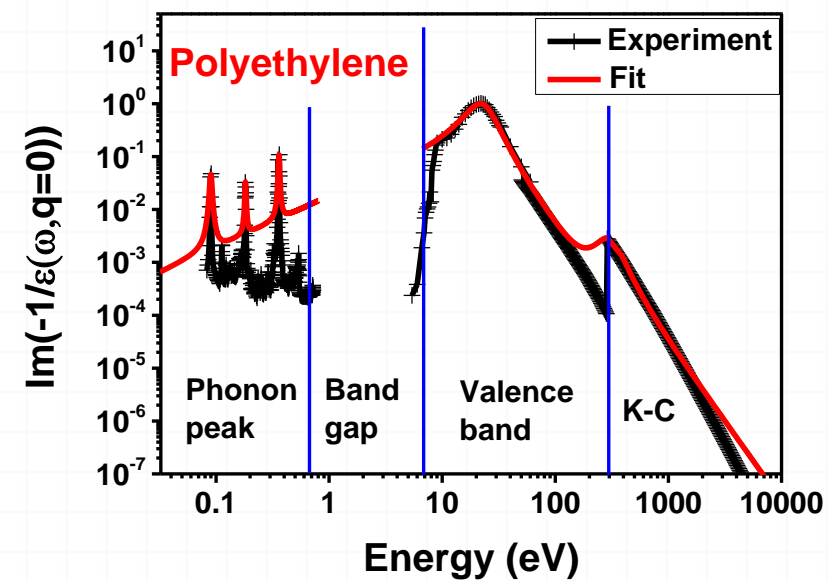
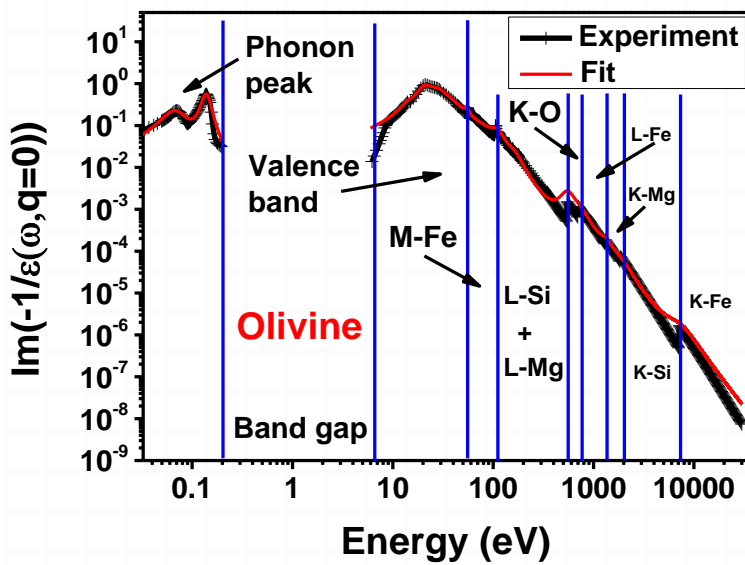
1. SHI passage and generation of fast primary δ -electrons
2. $\sim 10^{-17}$ s Spreading of δ -electrons and secondary electron cascading. Creation of secondary electrons and holes
3. $\sim 10^{-16}$ - 10^{-14} s Kinetics of all next generations of electrons and holes
4. $\sim 10^{-14}$ s Auger decays of deep shell holes $\sim 10^{-15}$ s
5. Radiation decay and photons transport

Complex Dielectric Function

e.g. Ritchie and Howie formalism

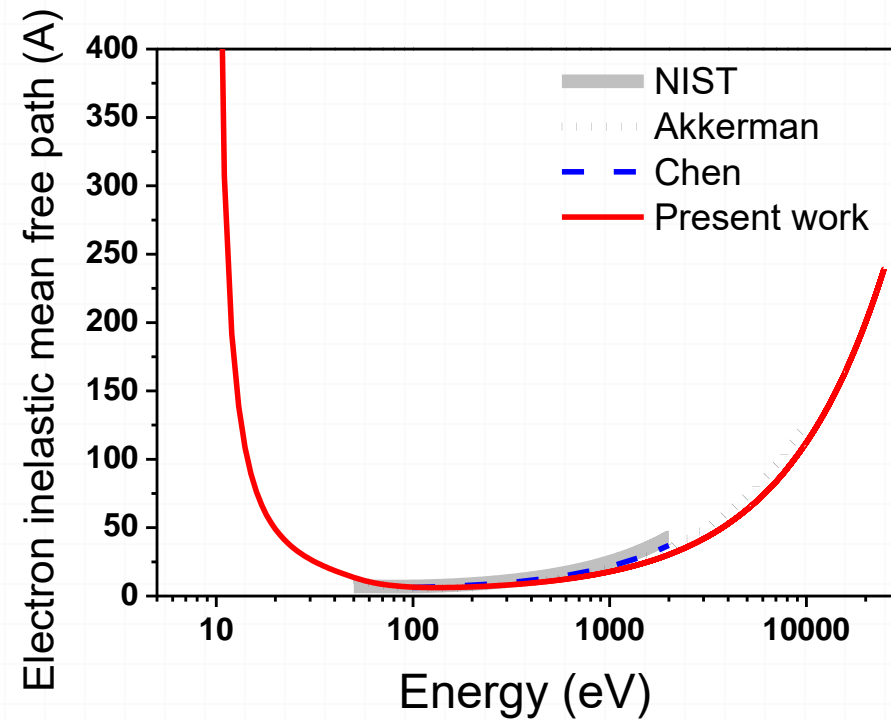
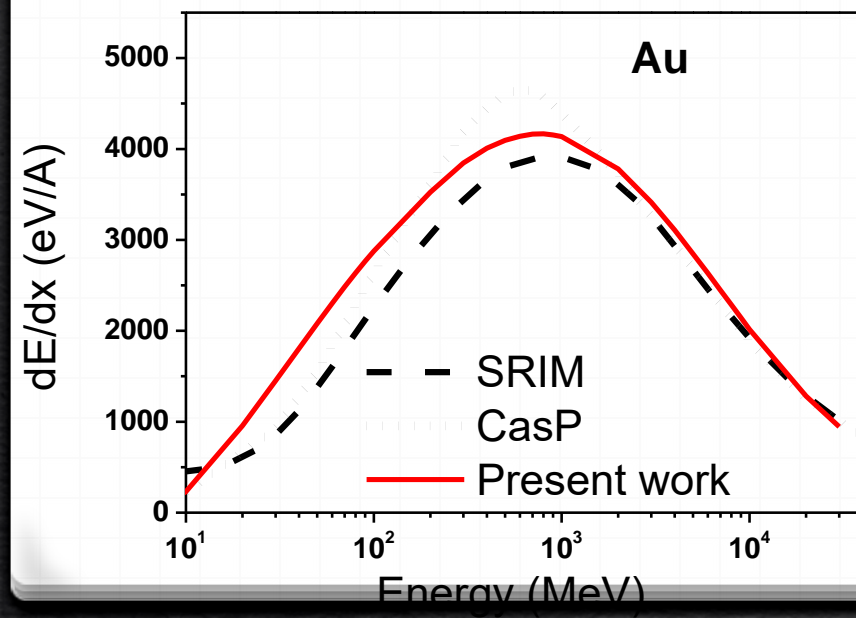
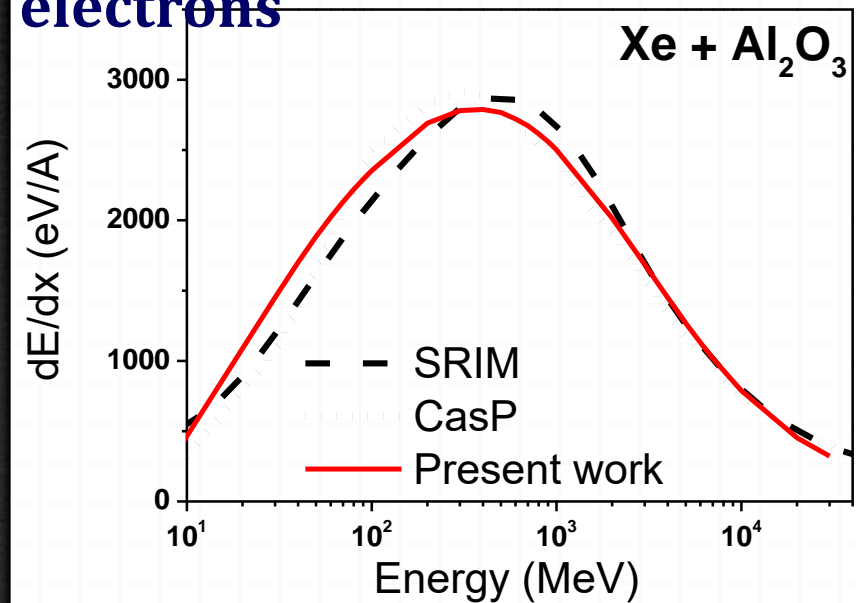
- individual scattering: ionization of the valence band or deep shells
- collective scattering: plasmons, phonons etc.

$$\frac{\partial^2 \sigma_{el}}{\partial k \partial(h\omega)} \sim \text{Im} \left[\frac{-1}{\varepsilon(\omega, q)} \right] = \sum_{i=1}^{n^{os}} \frac{A_i \gamma_i h\omega}{[h^2 \omega^2 - (E_{0i} + h^2 q^2 / (2m_e))^2]^2 + (\gamma_i h\omega)^2}$$



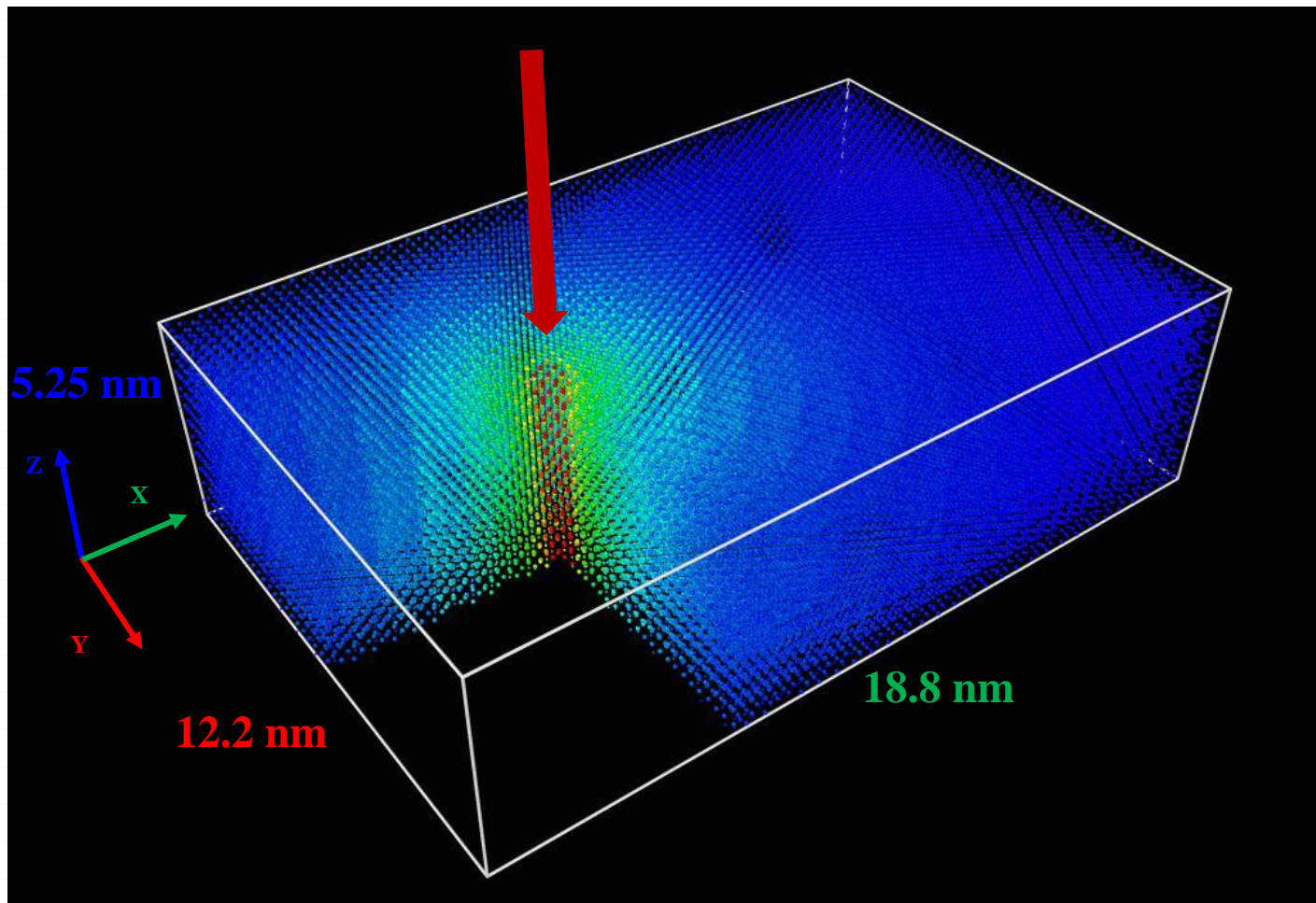
TREKIS: Verification of model

Electronic energy loss of ions and inelastic mean free paths of electrons

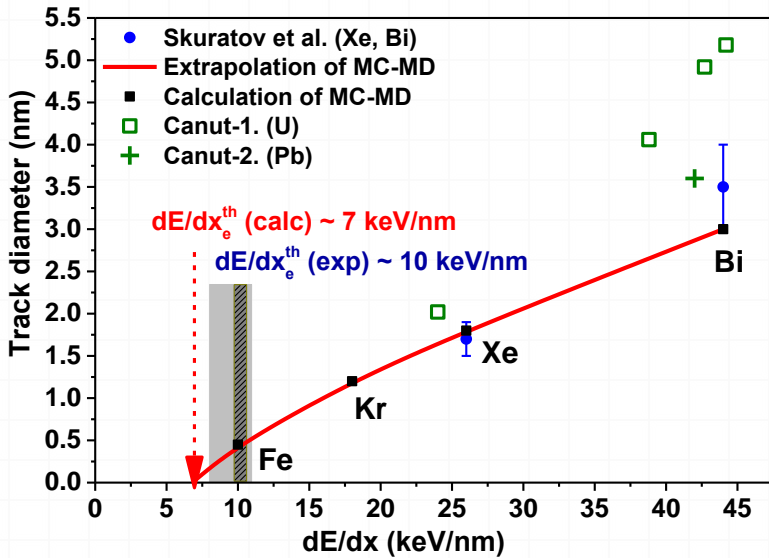


Good coincidence with SRIM,
CasP and NIST database

MC TREKIS + MD LAMMPS

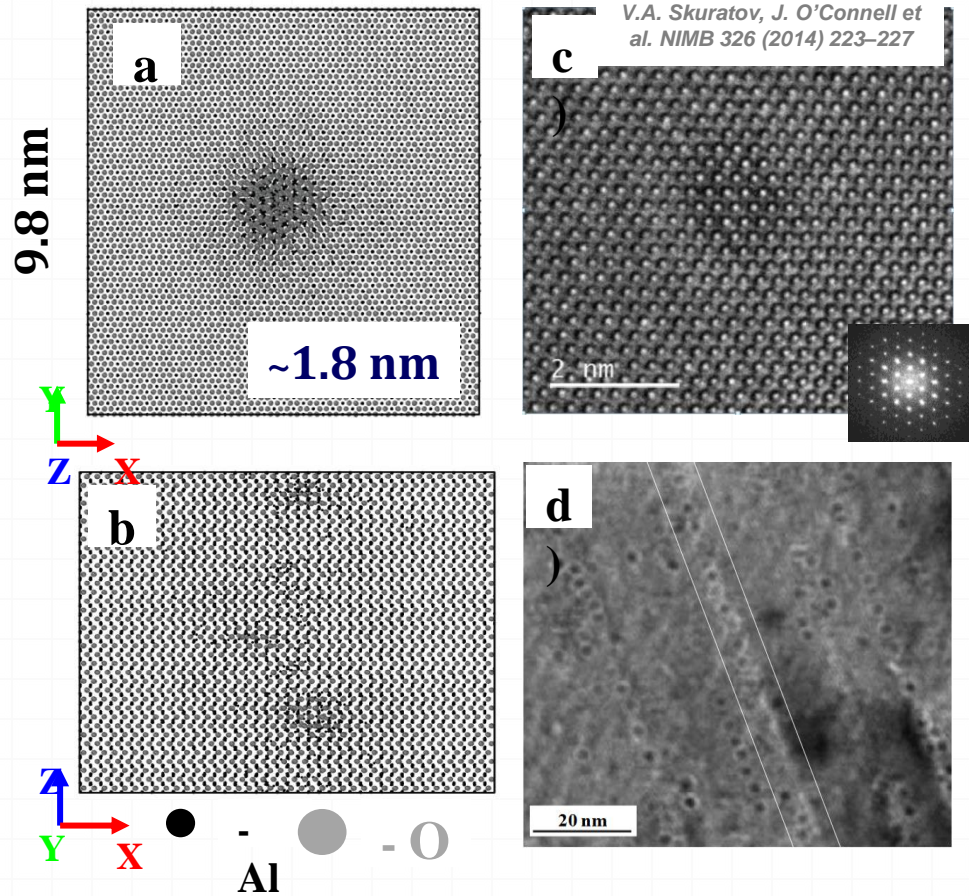


Threshold and morphology of tracks in Al_2O_3



$$(dE/dx)^{th} \sim 7 \text{ keV/nm}$$

$$(\sim 3.2 \pm 0.4 \text{ eV/atom})$$

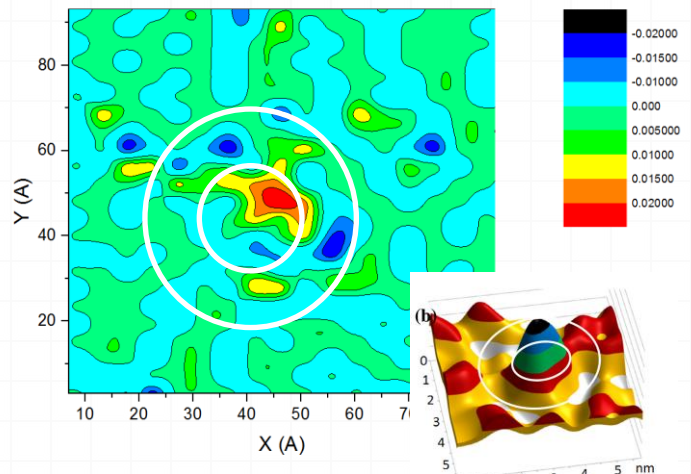


167 Mev Xe
Crystalline damaged
discontinuous track of 1.8
nm diameter after 50 fs

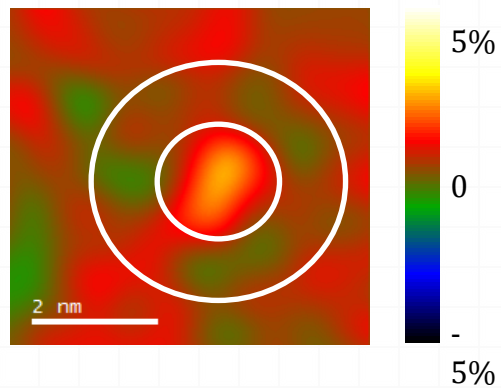
Residual strain of Xe 167 MeV track in Al_2O_3

Lattice deformation:

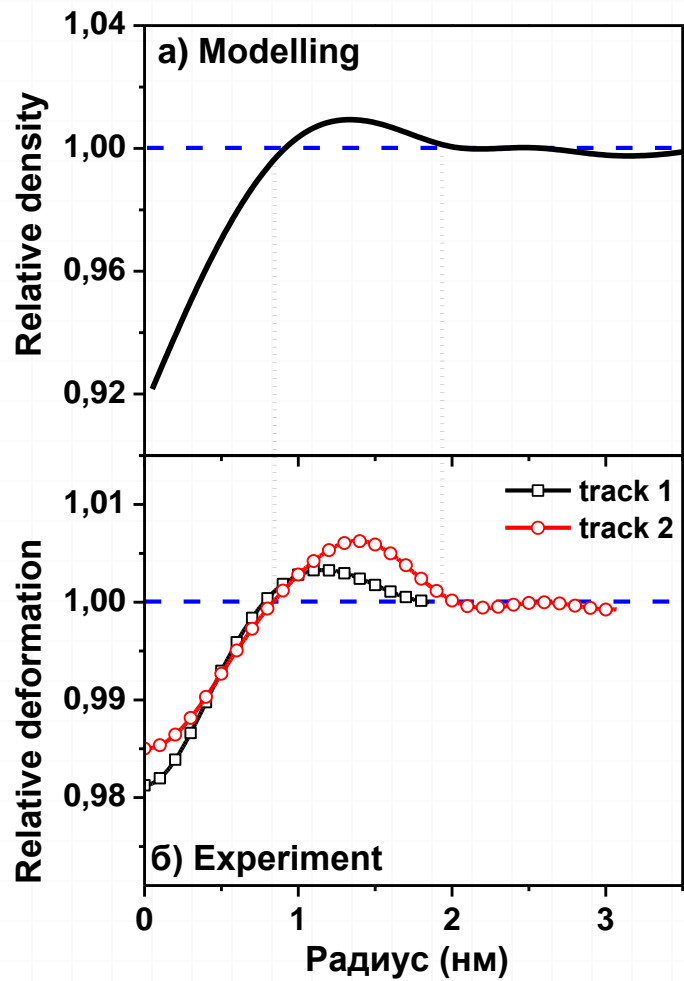
Simulations



Experiment

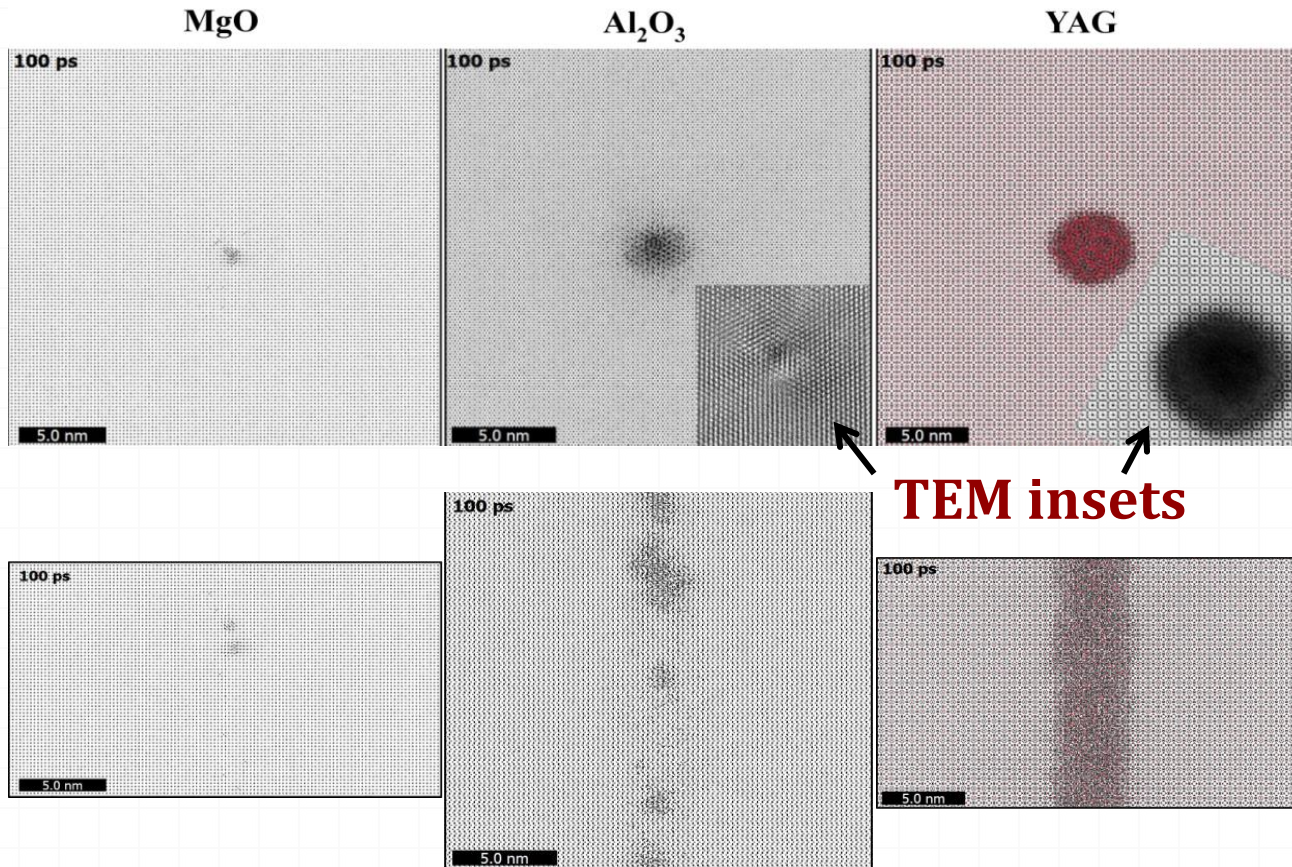


Radial density of Al_2O_3



underdense core is surrounded by overdense shell

Recrystallization of tracks in different dielectrics



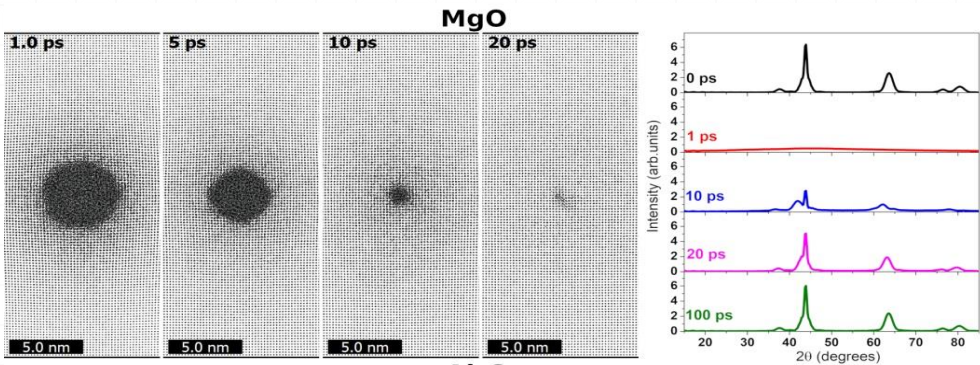
MgO - only point defects were created

Al₂O₃ - crystalline discontinuous track of D ~ 2 nm

YAG - continuous amorphous track of D ~ 6.5 nm

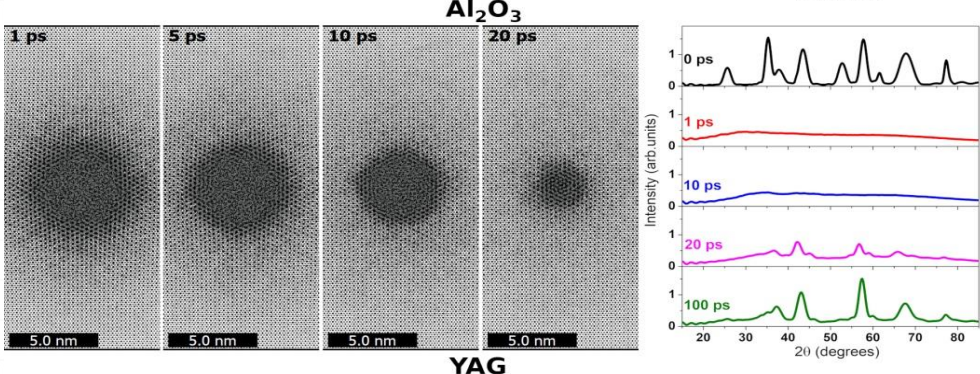
Recrystallization plays a crucial role for track formation in MgO, Al₂O₃ and YAG

MgO



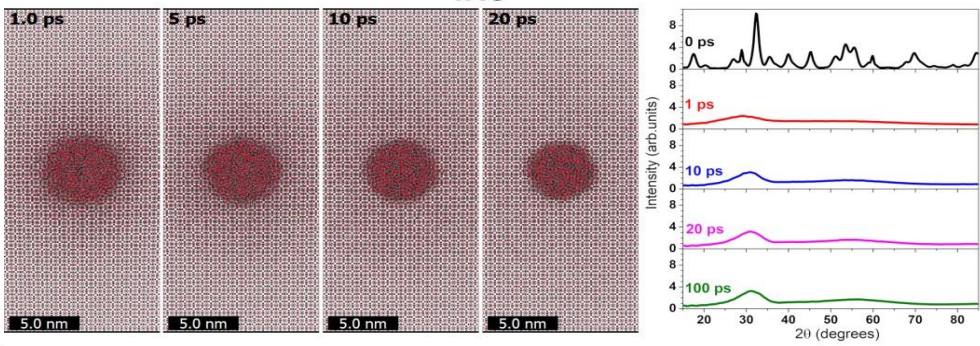
nearly perfect
recrystallization

Al₂O₃



partial recovery

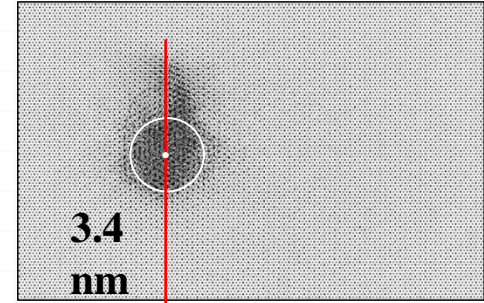
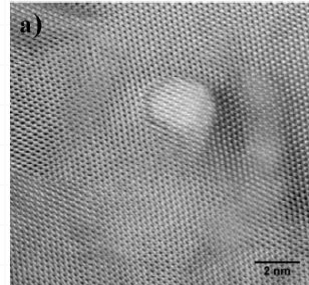
YAG



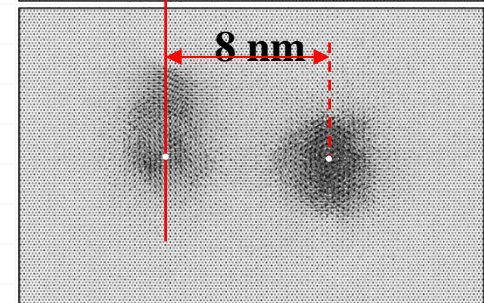
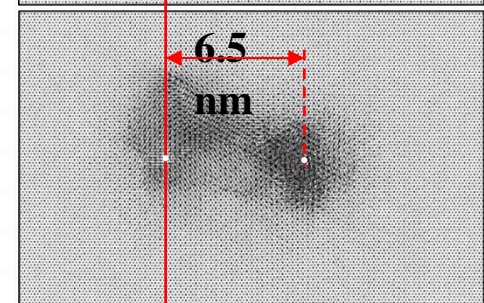
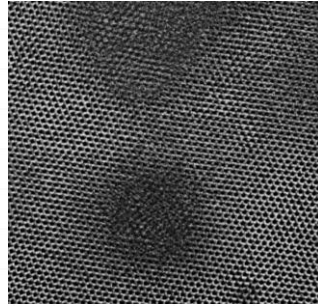
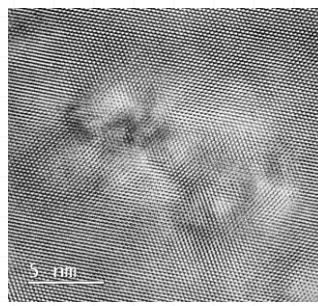
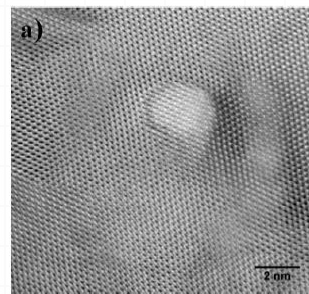
almost no recovery

Overlapping of SHI tracks.

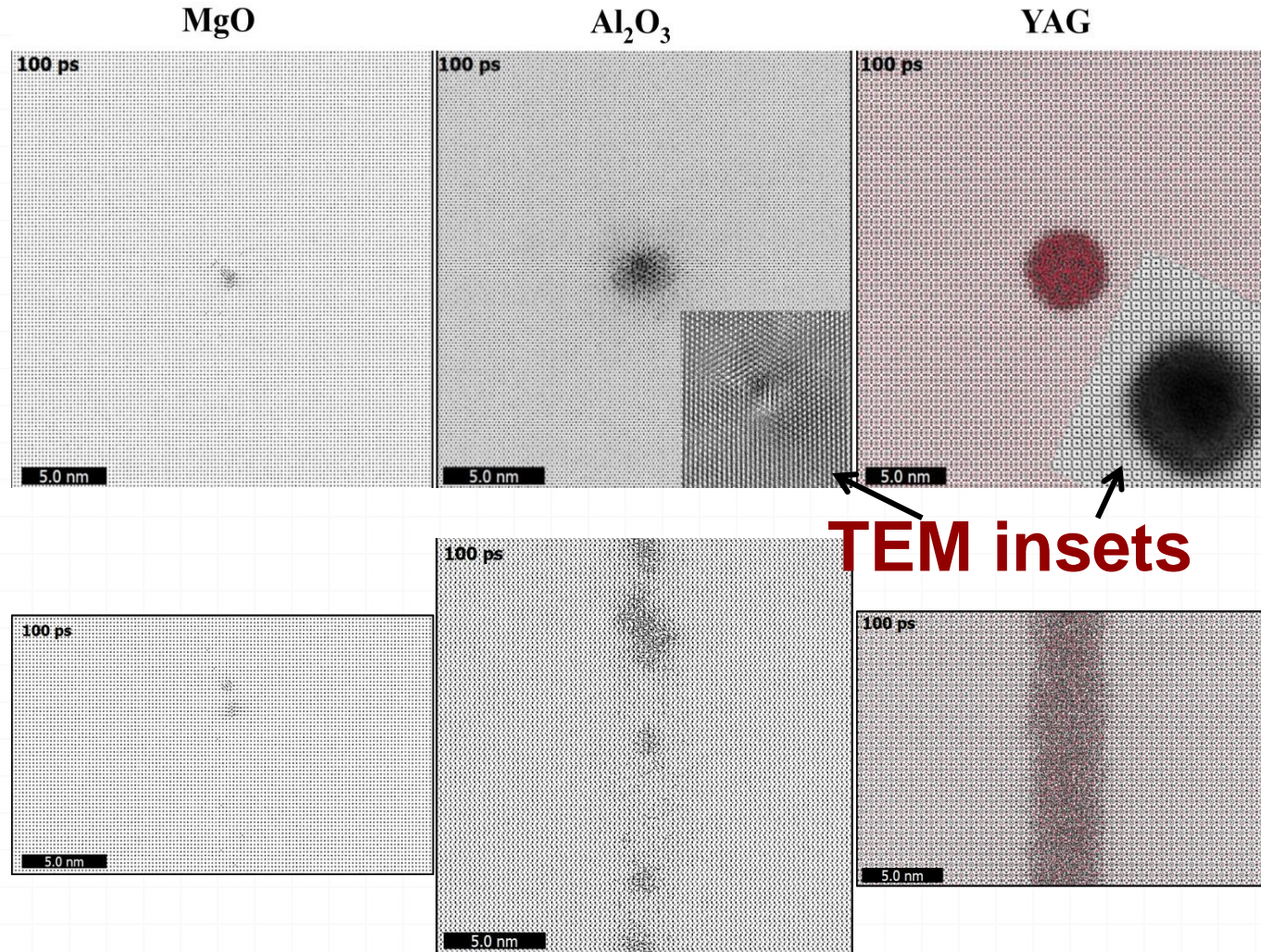
Bi 700 MeV in Al_2O_3



- Second ion causes annealing of defects created by the first one
- Ions at longer distances cause partial annealing of older tracks
- Radius of recovery is ~ 6.5 nm (experimental ~ 5.4 nm) corresponding to the track density of $\sim 2.7 \times 10^{12} \text{ cm}^{-2}$



Recrystallization during track formation process



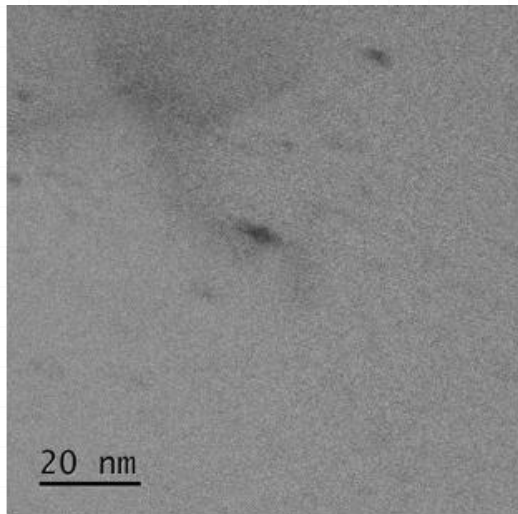
MgO - only point defects were created around the ion trajectory

Al₂O₃ - crystalline discontinuous track with the diameter about 2 nm

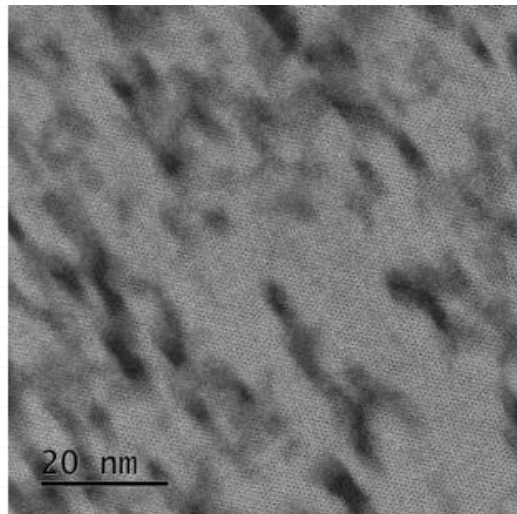
YAG - continuous amorphous track of ~6.5 nm in diameter

p-Si₃N₄ + Xe 220 МэВ

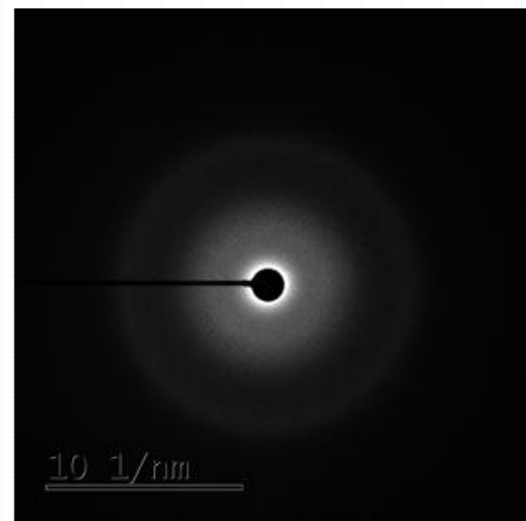
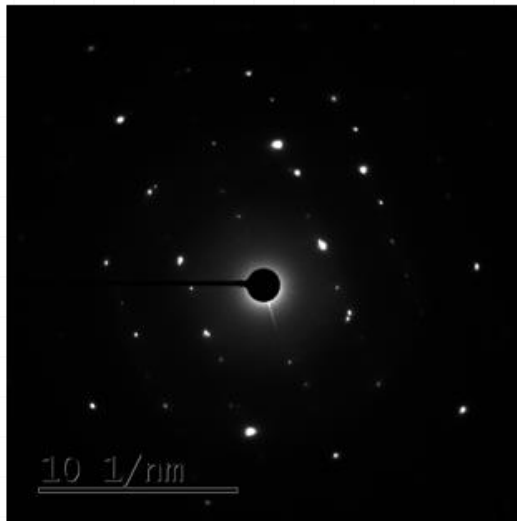
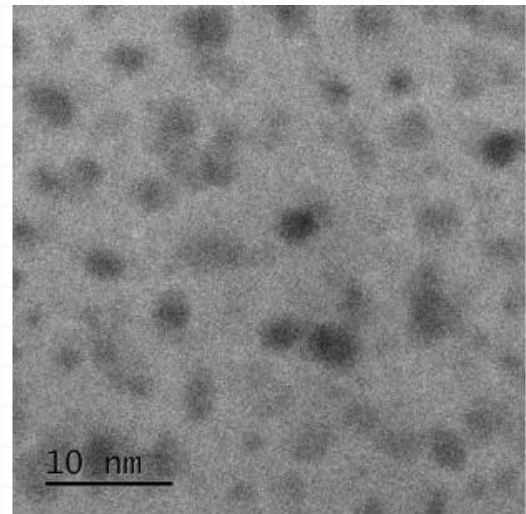
$5 \times 10^{11} \text{ cm}^{-2}$



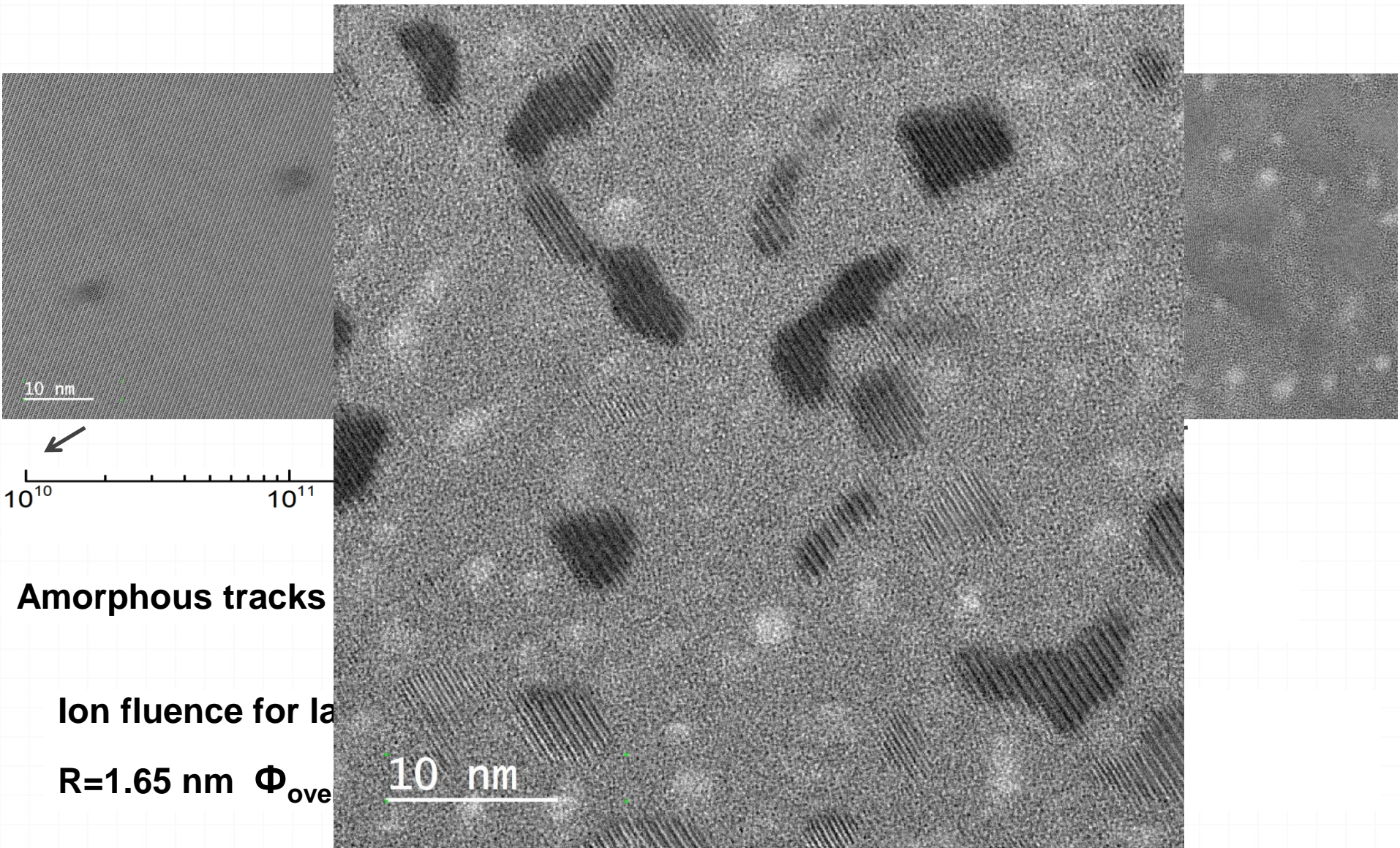
$1 \times 10^{13} \text{ cm}^{-2}$



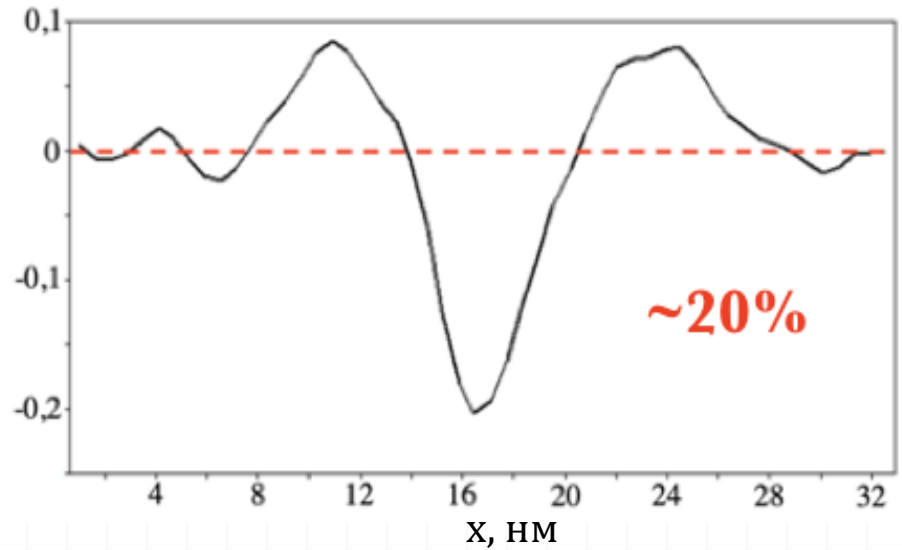
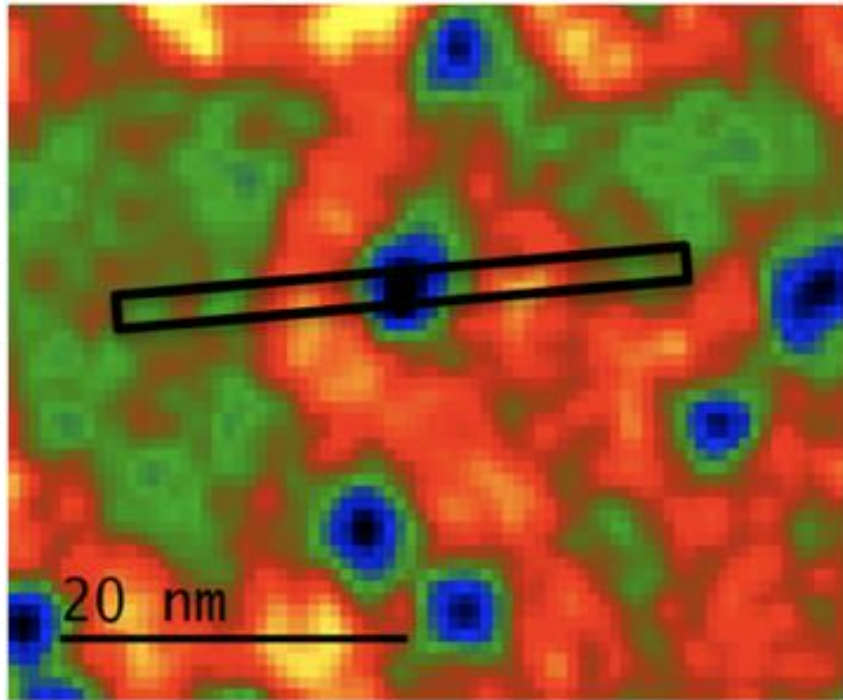
$2 \times 10^{14} \text{ cm}^{-2}$



$\text{Si}_3\text{N}_4 + \text{Bi}$, 700 MeV

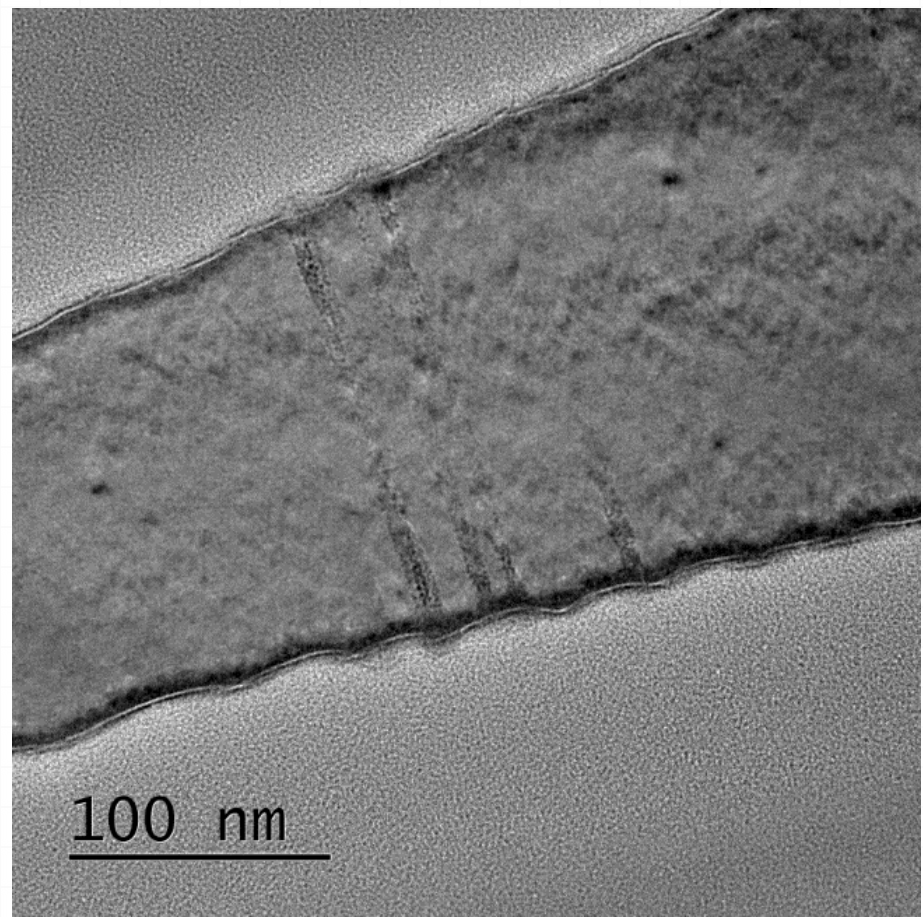
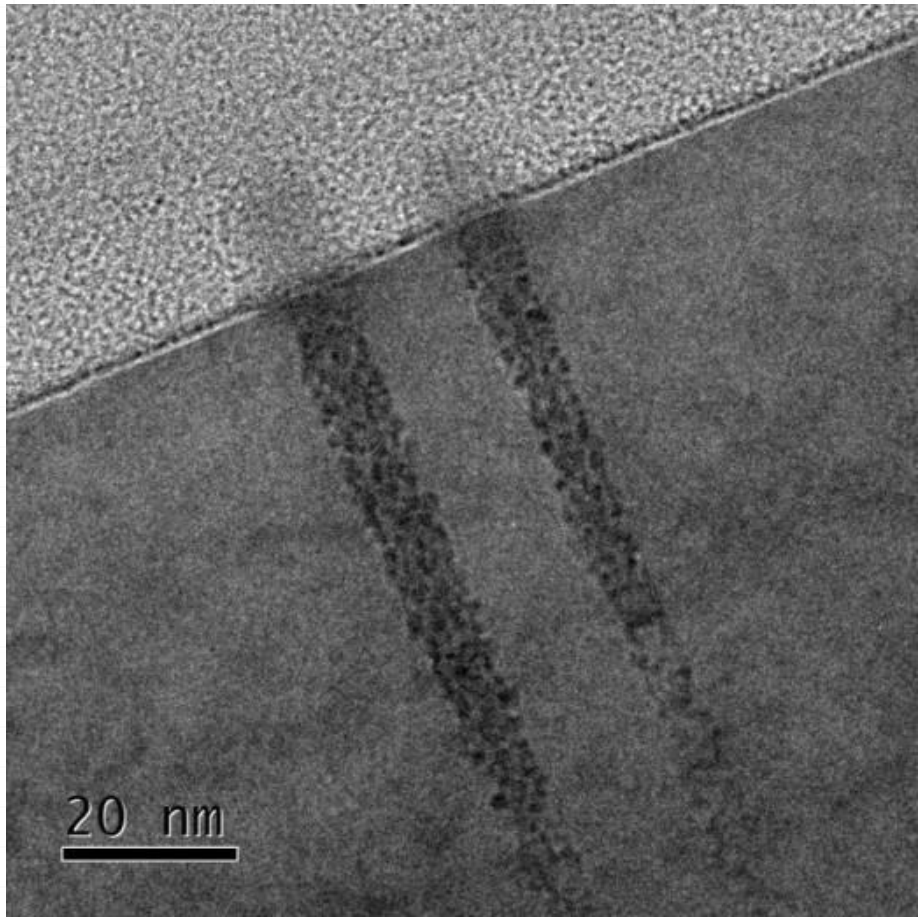


a-Si₃N₄ + Bi 710 МэВ, 5x10¹⁰ см⁻²



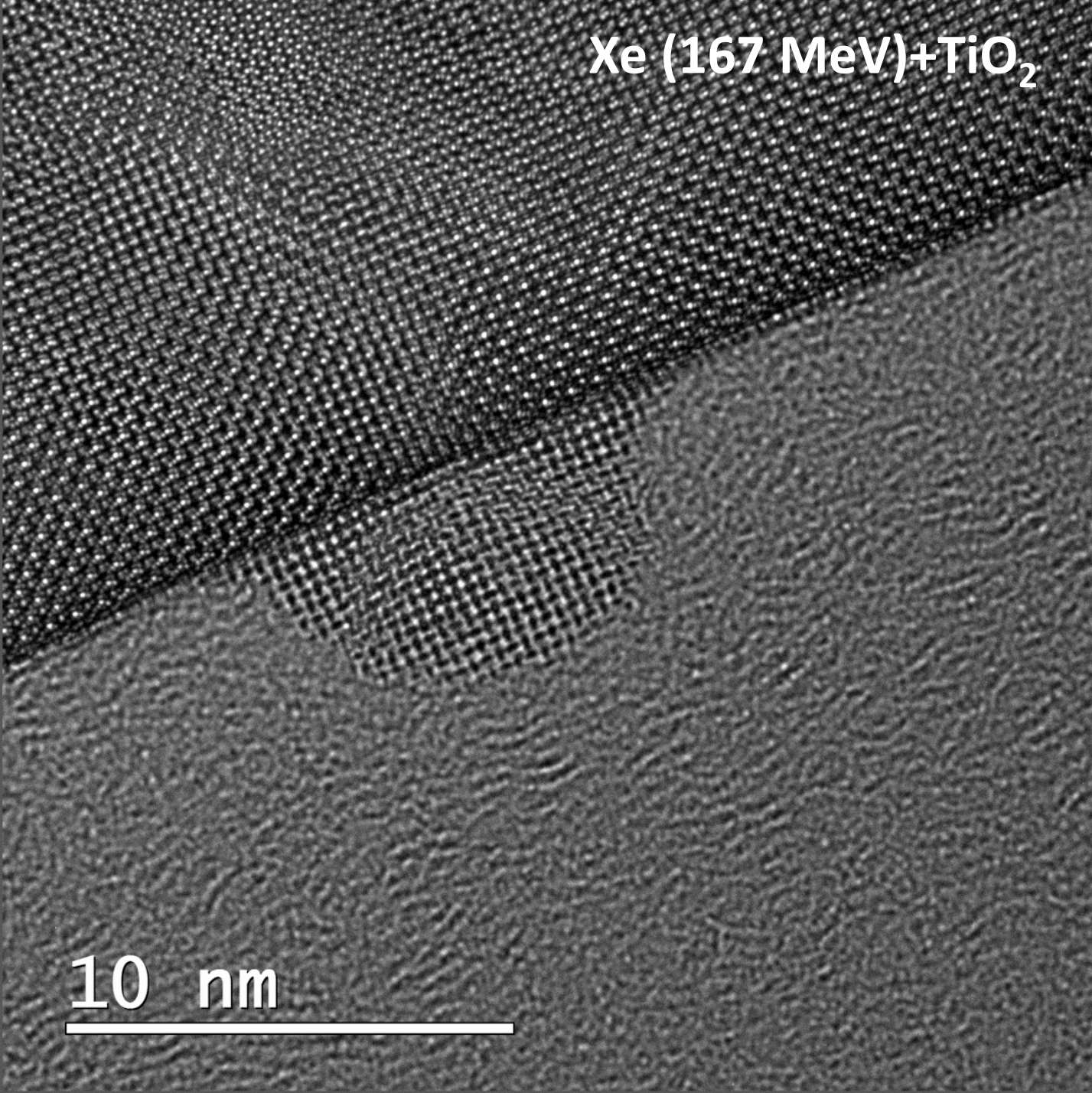
Radial density of Si₃N₄

Surface effects of dense ionization in ceramics and oxides

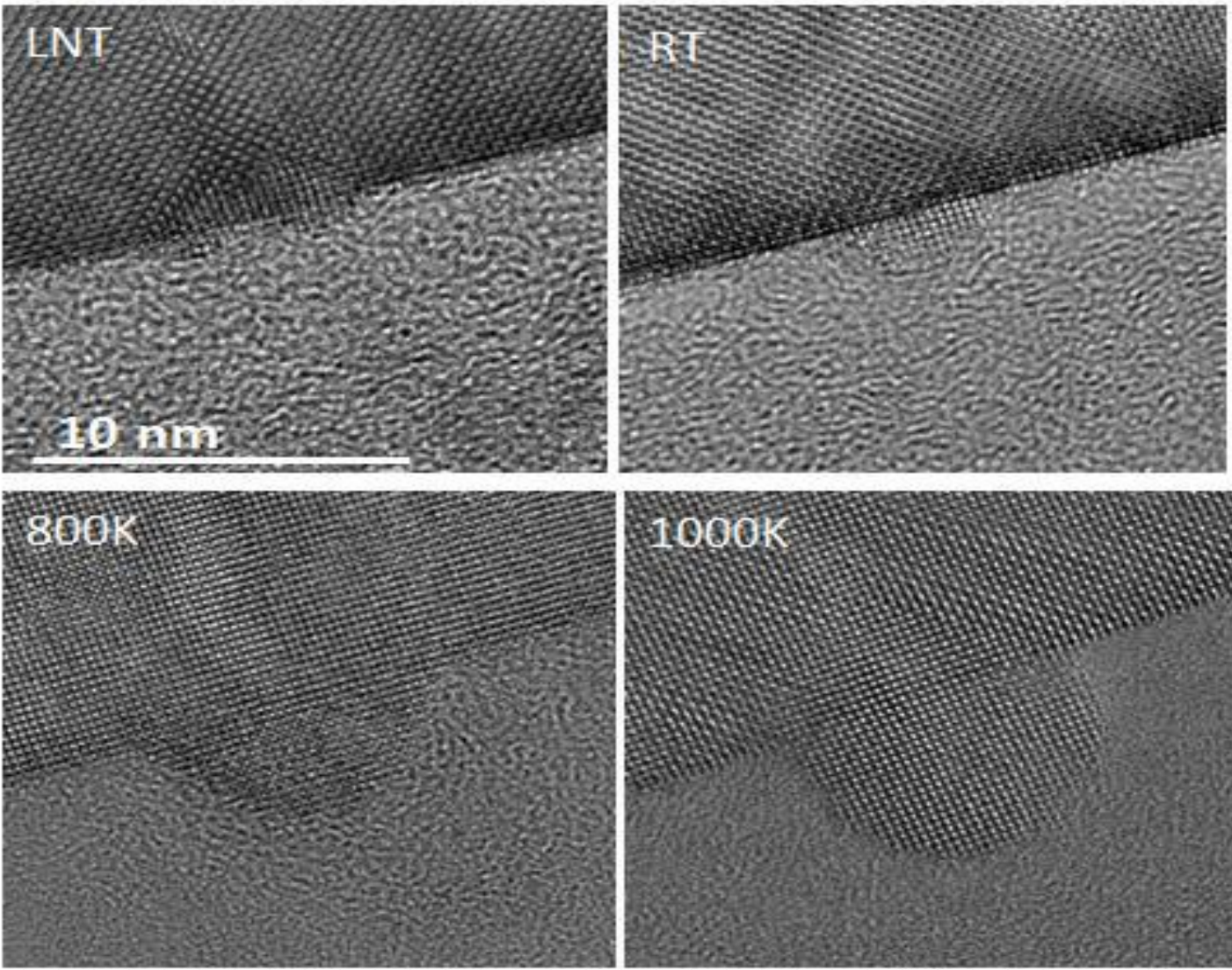


167 MeV Xenon ion induced hillocks in TiO_2

Xe (167 MeV)+TiO₂



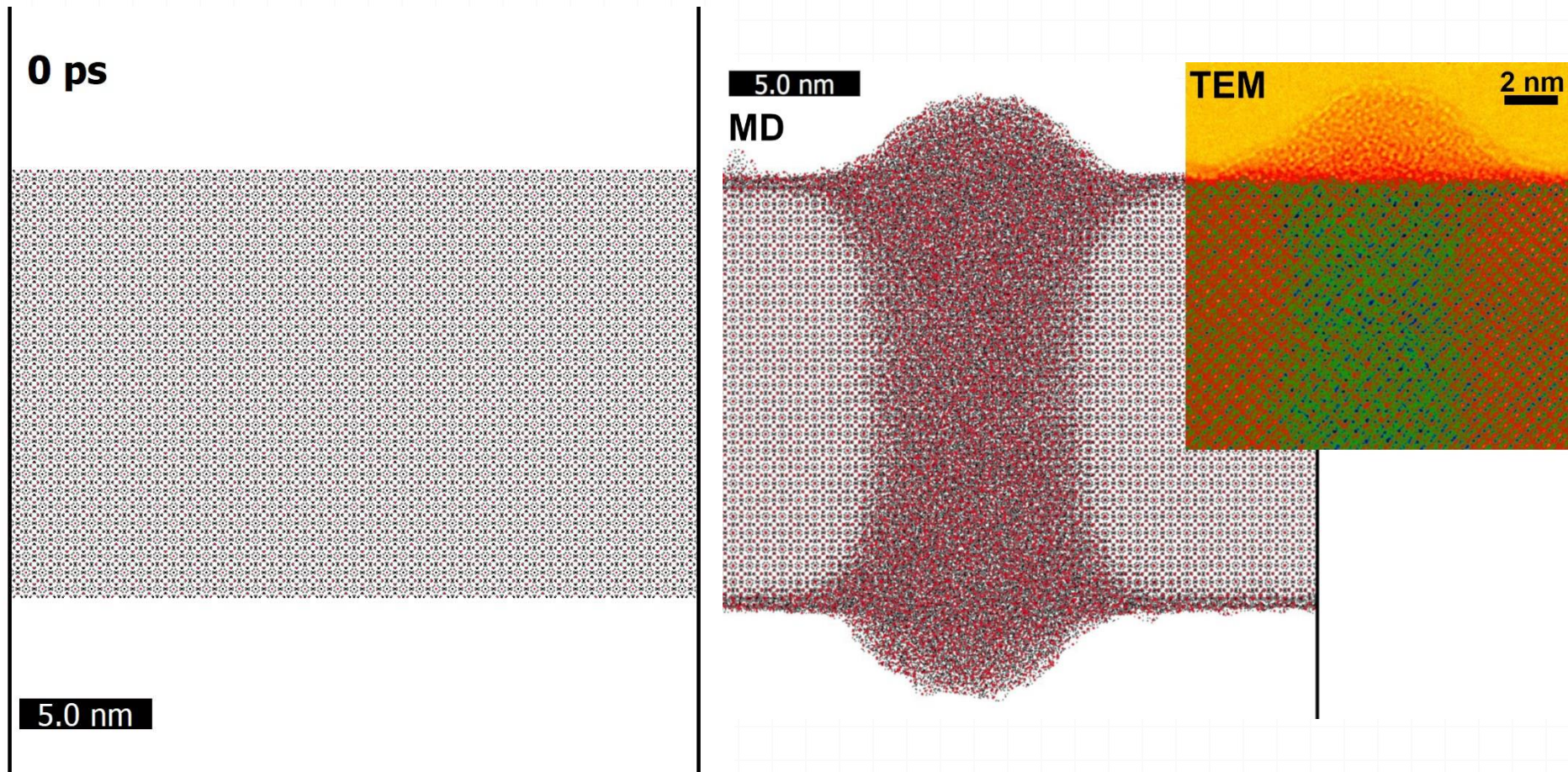
Surface effects of dense ionization in ceramics and oxides



Xe (220 MeV) + TiO_2 : Hillock size vs irradiation temperature

Amorphous hillocks in YAG

Bi 700 MeV ion



YAG demonstrates almost no damage recovery:
amorphous cylindrical track and amorphous hillock

Thank you for your
attention!